REPORT DOCUMENTATION PAGE

Form Approved
OMB No. 0704-0188

1. REPORT DATE *(DD-MM-YYYY)*	**2. REPORT TYPE**	**3. DATES COVERED** *(From - To)*
20-06-2012	Technical Paper	

4. TITLE AND SUBTITLE

Accuracy analysis of DSMC chemistry models applied to a normal shock wave

5a. CONTRACT NUMBER

5b. GRANT NUMBER

5c. PROGRAM ELEMENT NUMBER

6. AUTHOR(S)
S. Gimelshein, I. Wysong, Y. Bondar, M.Ivanov

5d. PROJECT NUMBER

5f. WORK UNIT NUMBER
23080532

7. PERFORMING ORGANIZATION NAME(S) AND ADDRESS(ES)

Air Force Research Laboratory (AFMC)
AFRL/RQRA
10 E. Saturn Blvd.
Edwards AFB CA 93524-7680

8. PERFORMING ORGANIZATION REPORT NUMBER

9. SPONSORING / MONITORING AGENCY NAME(S) AND ADDRESS(ES)

Air Force Research Laboratory (AFMC)
AFRL/RQR
5 Pollux Drive
Edwards AFB CA 93524-7048

10. SPONSOR/MONITOR'S ACRONYM(S)

11. SPONSOR/MONITOR'S NUMBER(S)
AFRL-RZ-ED-TP-2012-219

12. DISTRIBUTION / AVAILABILITY STATEMENT

Approved for public release; distribution unlimited (PA #12470).

13. SUPPLEMENTARY NOTES
For presentation at the Rarefied Gas Dynamics Conference, Zaragosa, Spain, 9-13 July 2012.

14. ABSTRACT

A preliminary validation study of three DSMC chemistry models, two recent and one standard, is presented. First the 2D geometry and numerical approach used to simulate the shock experiments is verified. Next, 2 different vibrational relaxation models are validated by comparison with data for the M=9.3 case where dissociation is small in the nonequilibrium region of the shock. Finally, the 3 DSMC chemistry model results are compared for the M=13.4 case where nonequilbrium dissociation (in the region where the vibrational temperature is greatly different for the rotational and translational temperature) is important. It is shown that the peak vibrational temperature is very sensitive to vibrational favoring in the chemistry model and that the vibrationally-favored KSS model predicts the measured peak quite well.

15. SUBJECT TERMS

16. SECURITY CLASSIFICATION OF:			**17. LIMITATION OF ABSTRACT**	**18. NUMBER OF PAGES**	**19a. NAME OF RESPONSIBLE PERSON**
					A. Ketsdever
a. REPORT	**b. ABSTRACT**	**c. THIS PAGE**			**19b. TELEPHONE NUMBER** *(include area code)*
Unclassified	**Unclassified**	**Unclassified**	SAR	8	N/A

Accuracy Analysis of DSMC Chemistry Models Applied to a Normal Shock Wave

Sergey Gimelshein*, Ingrid Wysong†, Yevgeny Bondar** and Mikhail Ivanov**

*ERC Inc, Edwards AFB CA 93524
†Propulsion Directorate, Edwards AFB, CA 93524
**Institute of Theoretical and Applied Mechanics, Novosibirsk, Russia

Abstract.
A preliminary validation study of three DSMC chemistry models, two recent and one standard, is presented. First the 2D geometry and numerical approach used to simulate the shock experiments is verified. Next, 2 different vibrational relaxation models are validated by comparison with data for the M=9.3 case where dissociation is small in the nonequilibrium region of the shock. Finally, the 3 DSMC chemistry model results are compared for the M=13.4 case where nonequilbrium dissociation (in the region where the vibrational temperature is greatly different for the rotational and translational temperature) is important. It is shown that the peak vibrational temperature is very sensitive to vibrational favoring in the chemistry model and that the vibrationally-favored KSS model predicts the measured peak quite well.

Keywords: DSMC method, chemical reactions, vibrational relaxation, normal shock wave
PACS: 51.10.+y, 82.20.Pm

INTRODUCTION

Modeling of chemical reactions in the direct simulation Monte Carlo (DSMC) method [1] has a 40-year long history. Starting from the simplest model with the probability described by a Heaviside step function and depending only on the line-of-centers collision energy, reaction models have grown over the years in their physical adequacy and sophistication. Many of them include such features as vibrational favoring and discrete internal energy modes. Nevertheless, the total collision energy (TCE) model [2] is still the most widely used chemical reaction model in the DSMC community. In the broader research field of non-equilibrium chemistry modeling in general, much effort and attention has been devoted to so-called vibration-dissociation coupling and to vibrational favoring of diatomic dissociation reactions. Although a number of reasonable models for both DSMC and continuum reacting flowfield simulations have been proposed, progress has been greatly hampered by a dearth of experimental data for non-equilibrium conditions that is of sufficient detail to distinguish between models. Most comparisons for proposed models have been with other models' predictions or with QCT (or similar) theoretical predictions for state-specific rates, state-specific cross sections, or two-temperature (2T) rates.

The present preliminary study is motivated by valuable recent measurements from Ibraguimova et al. [3, 4] which provide accurate vibrational temperatures of O_2 in a shock under non-equilibrium conditions. In addition, the data provide dissociation rate coefficients at high temperatures with various ratios of T_v/T, thus allowing both two-temperature values and reasonable extrapolations to the equilibrium values for the limit $T_v \to T$. The present objective is to provide a DSMC simulation of the shock cases and to allow the measurements to validate and distinguish between some key models.

NUMERICAL MODELS

The DSMC code SMILE [5] is used with the VHS collision model for intermolecular collisions. Since the focus here is high-temperature reacting flows, such as in a bow shock, VHS parameter values are selected that are reasonable for the high-temperature regime for the collision pairs (O_2-O_2 and O_2-O) of interest. Literature predictions for the viscosity of air species-pairs by Capitelli [6] are used, and VHS parameters that match the defined viscosity in the 2,000 K to 10,000 K range are selected (see Table 1). Note that though a reference temperature of $T_{ref} = 273$ K is used for convenience (since many DSMC codes use this T_{ref} value), the values of selected reference diameter d_{ref} and the

TABLE 1. High temperature VHS parameters for oxygen collisions. Upper numbers, d_{ref} in Å, lower numbers, ω.

	O	O_2
O	3.458	3.442
	0.76	0.75
O_2	3.442	3.985
	0.75	0.71

exponent in the viscosity-temperature dependence ω produce the desired viscosity values at high temperatures and do not match known viscosities at lower temperatures.

A discrete description of rotational and vibrational energies [7] is used. The rotational relaxation is done with the Larsen-Borgnakke (LB) model and assuming a temperature dependent rotational relaxation number [7] based on Parker expression [8]. Two different vibrational energy relaxation models are used. Both use anharmonic oscillator (AHO) energy levels. The first model, called LB hereafter, redistributes energy between translational and vibrational modes according to the Larsen-Borgnakke principle [9, 10], with the temperature-dependent vibrational relaxation number Z_{vib} defined to match the literature relaxation time temperature correlation for O_2 given in [11], with a high-temperature limit as per [12]. The second model, denoted QC, is a quasiclassical state-to-state vibrational relaxation model including both V-V and V-T transfers [13].

Three different DSMC models for chemical reactions were used. The first is the TCE model [2] with appropriate modifications [14] for quantized vibrational energy. The adjustable parameters used for the TCE model are: $A = 0.10547$ m^3/s, $B = -3.3999$, $E_a = 8.198 \times 10^{-19}$J, $\zeta = 2$ for O_2+O_2 dissociation reaction [3] and $A = 0.20637 \times 10^{-10}$ m^3/s, $B = -0.6828$, $\zeta = 2$ for O_2+O reaction. These ensure that the model would reproduce the reaction rate coefficient k_d in the equilibrium limit in the range 5000-15,000 K. The second is the Quantum Kinetic (QK) model, which has been discussed in some detail elsewhere [15, 16]. As has been shown, the QK model provides a very reasonable match with known dissociation rate coefficients at equilibrium without an a priori knowledge of the Arrhenius values. In this case, the O$-$2-O_2 equilibrium dissociation rate coefficient from [4] is assumed to be 2×10^{-19} m^3/s at 5000 K and 7^{-18} m^3/s at 10,000K ; the QK prediction using the present VHS collision parameters is 9^{-20} m^3/s at 5000 K and 2^{-18} m^3/s at 10000K. Note that the QK for the present work was modified for use with AHO energy levels for consistency (indications show that differences in the results based on the SHO level scheme are very minor). The third model [17] provides a DSMC implementation of a literature two-temperature kinetic model [18]. Here again the model parameters as defined so as to match the TCE model and measured rates [4] in the equilibrium limit.

The key feature of the state-specific model [17] is that it uses vibrational favoring. Unlike the TCE and QK models, where two collision pairs that have the same total energy ($E_{tr} + E_{vib} + E_{rot}$ for TCE and $E_{tr} + E_{vib,1}$ for QK) but different initial vibrational energy (or level v) (i.e., collision 1 has high v but low E_{tr} while collision 2 has low v but high E_{tr}) will have the same probability of reaction, the state-specific model considers the initial vibrational level in addition to the total energy, so collisions 1 and 2 would have very different reaction probabilities. Note that a number of previous DSMC chemistry models [19, 20] have also included this favoring effect in various ways.

Recombination reactions are not presently included. Because of the low pressures and the short post-shock times relevant to the measurements, recombination is believed to have a negligible effect, but further work is needed to test this assumption.

FLOW CONDITIONS

The two shock conditions simulated here are based on two cases from the measurements in Ref. [4]. Both have an inflow of pure O_2 at T=295K. The low-speed case has initial velocity of 3.07 km/s (Mach number M=9.3) and the high-speed case has initial velocity of 4.44 km/s (M=13.4). The corresponding gas pressures are 2 torr and 0.8 torr. In order to simulate the normal shock wave and relaxation front measured in a shock tube, the present study uses a planar 2D configuration, with the free stream conditions corresponding to the experimental ones, and a shock wave formed by the interaction of the hypersonic gas flow and a rectangular body. To minimize the impact of the body, specular reflection of gas molecules on the wall is assumed, and a very small Knudsen number of about 2×10^{-4} is used. The full size of the rectangle in the direction perpendicular to the flow is 12 cm and 30 cm for M=9.3 and 13.4,

respectively, although only half of the body was modeled due to the symmetry of the problem.

Sensitivity study of modeling results to the numerical parameters of the approach has been conducted. Convergence of results in terms of the number of simulated particles and collision cells was achieved for a total of about 80 million particles and 7 million cells. The average number of particles in a volume with a linear size of the gas mean free path, λ^3, was about 3, which was shown in an earlier work [22] to be sufficient for modeling shock waves. An example of the grid and particle convergence study is shown in Fig. 1 (left) that also illustrates the computational domain used in this work. It is clearly seen that the vibrational temperature field (as well as other gas properties, not shown here) agree for the baseline model, upper half of the figure, and a case where two times more particles in a λ^3 volume and two times finer collision cell size was used, lower half of the figure. The impact of the Knudsen number was also tested, and the results are summarized in Fig. 1 (right). The profiles of the total gas number density and O_2 vibrational temperature along the stagnation streamline for the baseline Knudsen number and $Kn \approx 10^{-4}$ show that virtually no difference is observed inside the shock and immediately after it. There is a very small difference between number densities further away from the shock, obviously related to the proximity of the wall in the baseline case, but the vibrational temperature is unaffected. All this indicates that the chosen 2D setup allows adequate comparison between computed vibrational temperatures along the stagnation streamline and normal shock wave measurements in a shock tube [4].

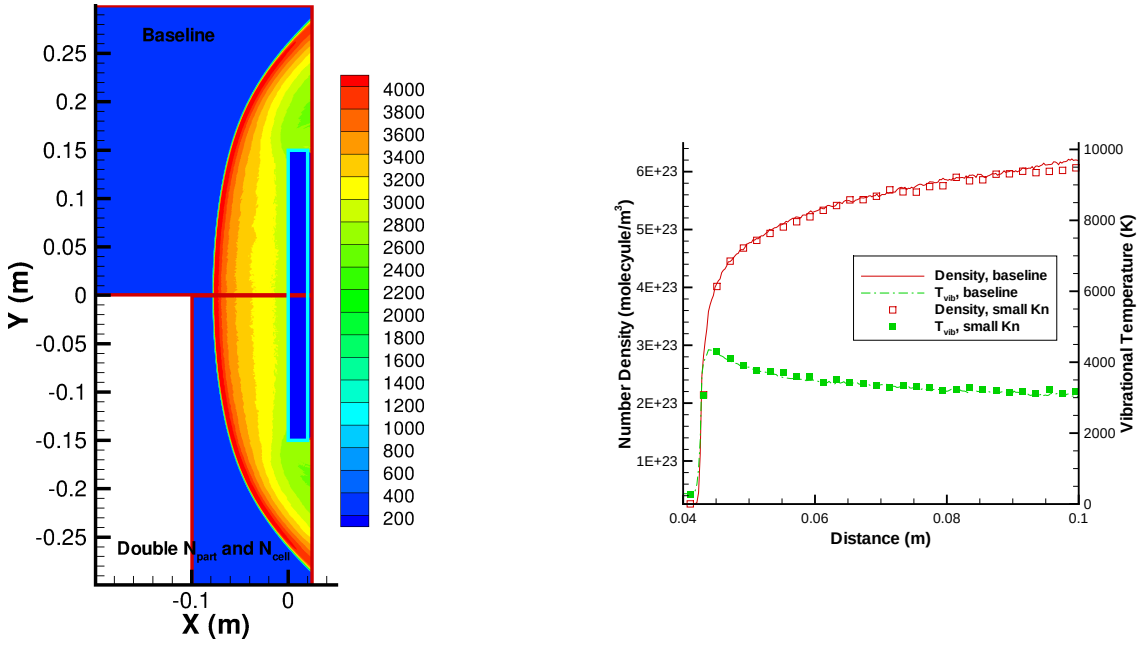

FIGURE 1. The impact of the number of particles and cells on vibrational temperature field (left) and of Knudsen number on gas properties along the stagnation streamline (right) for M=13.4 and LB/TCE models.

M=9.3 SHOCK WAVE

Consider first the flow of non-reacting molecular oxygen for M=9.3. In this case, the dissociation reactions were turned off, while all other conditions were the same as for the baseline M=9.3 flow. The profiles of gas macroparameters along the symmetry axis are presented in Fig. 2 (left). The gas mean free path λ in the free stream is about 0.02 m, and the distance of about 10λ from the shallow part of the shock to the peak translational temperature is consistent with a number of earlier studies of the normal shock wave structure [1]. The rotational relaxation time is on average only about a factor of five larger than the translational one, and thus the rotational temperature T_{rot} only slightly lags behind translational temperature T_{trn}. They equilibrate after the first 30λ of the shock front, and coincide after that. As expected, the vibrational relaxation is much slower than the relaxation of the other two modes; all three modes equilibrate after about $2{,}000\lambda$. It is important to note that even though a two-dimensional setup is used instead of a one-dimensional solution with exact Rankine-Hugoniot conditions for M=9.3, the mode temperatures after the shock for a plateau at a value of about 4,400 K, which agrees with the Rankine-Hugoniot solutions for a variable specific heat ratio with the number of vibrational degrees of freedom ξ_{vib} defined by the expression for a simple harmonic

oscillator, $\xi_{vib} = \frac{2\theta_{vib}/T}{\exp(\theta_{vib}/T)-1}$. Here, θ_{vib} is the vibrational characteristic temperature, and T is the gas temperature. The gas bulk velocity in the free stream direction, U_x, reaches its Rankine-Hugoniot value of about 360 K in the region where the mode temperatures merge. After that, the velocity almost linearly decreases to 0 at the stagnation point at $X = 0$. The decrease is fairly slow as the region between the shock and the body is much noticeably than the thickness of the shock front. Generally, these results once more confirm that the impact of the body on the shock wave structure along the stagnation streamline is relatively small.

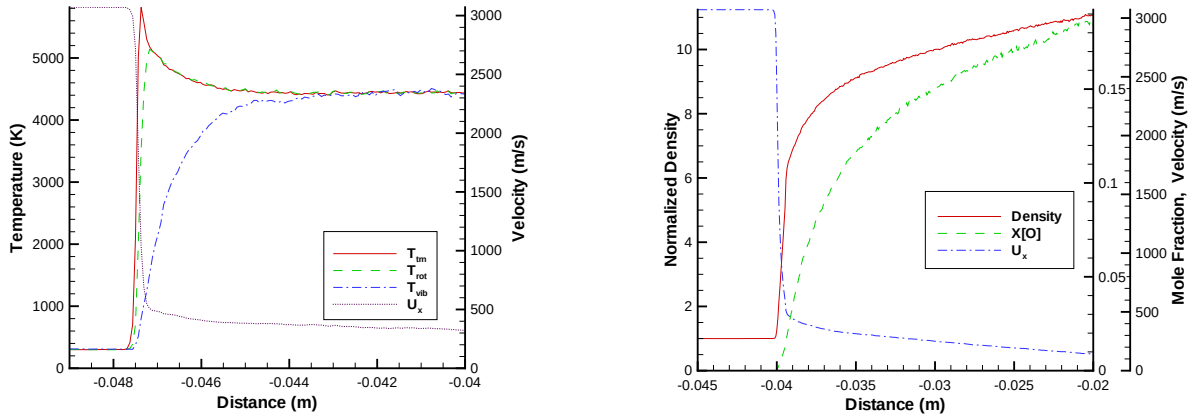

FIGURE 2. Gas properties along the stagnation streamline for non-reacting (left) and reacting (right) flow for the M=9.3 case. LB model of VT energy transfer and TCE model of chemical reaction.

The gas properties for the reacting flow are shown in Fig. 2 (right). In this case, the flow velocity profile is qualitatively similar, although with somewhat lower values immediately after the translation-rotation relaxation front than for the non-reacting flow. The major difference of the reacting flow is that there is no clear density plateau in the after-shock region. A fairly large number of dissociation reactions results in gradual increase in density between the shock front and the body (the density here is normalized by the free stream value). The increase in the number of dissociating oxygen molecules is illustrated by the atomic oxygen mole fraction, X[O], which rises from zero in the free stream to over 20% near the wall. Note also that even though the increase in X[O] is observed in the region of strong translation-rotational non-equilibrium, the number of reactions there is relatively small, and the gas properties to the left of the translational temperature maximum may be considered independent of chemical reaction. Comparison of translational temperatures for the reacting and non-reacting gases (cf. Fig. 2, left and Fig. 3, left) indicates that the chemical reactions lower the translational temperature peak by only about 200 K.

The impact of chemical reactions becomes more pronounced downstream, where the maximum rotational temperature decreases from almost 5,200 K for non-reacting case to about 4,800 K for reacting case. It is even more significant in the region of maximum vibrational temperature. Chemical reactions reduce that maximum by almost 800 K. The rotational relaxation length is virtually independent of the dissociation process, while the vibrational relaxation length somewhat increases in the reacting case, obviously, since the vibrational relaxation rate strongly increases with temperature. Since the TCE model does not include vibrational favoring, the dissociation modeled with TCE does not cause non-equilibrium between vibrational and translational modes. This is clearly seen in Fig. 3 (left): all mode temperatures are equal after they merge about 3 mm downstream from the vibrational temperature maximum. The slow decrease of gas temperature after that is related to the transfer of thermal and kinetic gas energy to the potential energy of newly created atoms.

The fact that the translational and internal temperatures are equal generally does not guarantee that the velocity/energy distribution of the corresponding modes is Maxwell/Boltzmann. In order to analyze how close the energy distributions to the equilibrium form, the computations included sampling of velocity and internal energy distribution functions. The computations showed that downstream from the point where the translational and rotational merge, the velocity distribution is Maxwellian in all directions, and the rotational energy distribution is Boltzmann. The vibrational distribution, however, to a large extent depends on the model used. An example is presented in Fig. 3 (right), where vibrational populations are presented for the LB and QC models in a location downstream of the point where the translational and rotational modes equilibrate. The TCE model of chemical reactions is used with both vibrational energy models. For comparison, the Boltzmann vibrational distribution functions at the corresponding vibrational

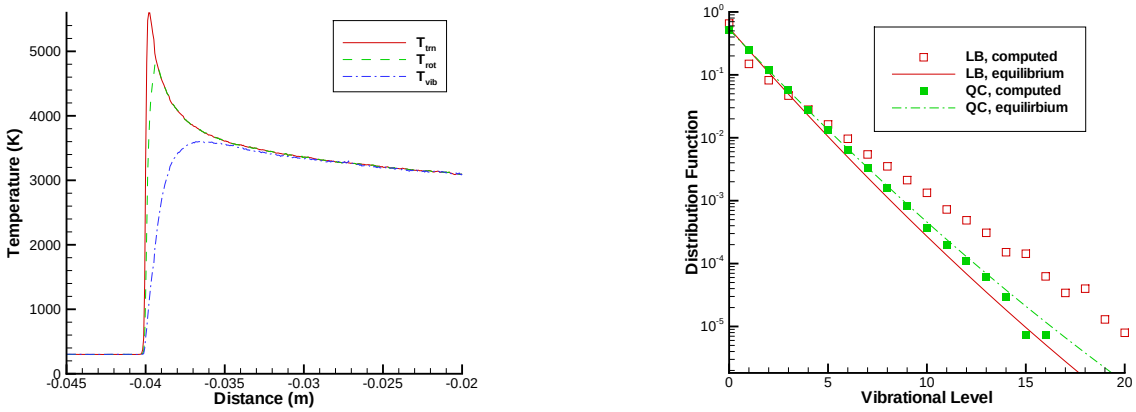

FIGURE 3. Temperatures of different modes for LB/TCE models at M=9.3 (left) and vibrational level populations for two vibrational energy transfer models.

temperatures are presented. It is clear that a strongly non-equilibrium vibrational population is obtained when the LB model is used, with underpopulated low (except for the ground state) and overpopulated high vibrational levels. The main reason for such a non-equilibrium is the lack of vibrational-vibration energy transfer, that was shown previously [20] to quickly equilibrate vibrational population in hypersonic flows. In the QC model, that takes into account both VT and VV energy transfer, the calculated vibrational distribution is close to Boltzmann.

Let us now analyze the impact of vibrational energy transfer and chemical reaction models on vibrational temperature along the stagnation streamline. Comparison of all cases considered for M=9.3 flow in presented in Fig. 4 (left). As before, the results are presented along the stagnation streamline, and the shift in X is related to different stand-off distances for different models (the wall is at X=0). The stand-off distance generally decreases as the number of dissociation reactions increases [21], and that is what observed in Fig. 4. The total number of reactions for the TCE model is about a factor of two larger than for the QK model, and the stand-off distance for the former is about 2.5 mm smaller. The maximum in vibrational temperature also strongly depends on the number of reactions. For the TCE model, it is about 200 K lower. Also note that the model of vibrational energy transfer, while only slightly changing the stand-off distance and the slope of the shock, does impact the maximum vibrational temperature. This is attributed to the fact that the LB model is characterized by strong non-equilibrium in the shock as compared to QC, and thus larger number of molecules with high vibrational energies. Even though the TCE and QK models do not have vibrational favoring, they are strongly influenced by the number of molecules with higher reaction energy (total in TCE and translation-vibration in QK). Thus more reactions occur inside the shock for the LB model, which lower the resulting vibrational temperature.

Comparison of numerical and experimental profiles of vibrational temperatures in shown in Fig. 4 (right). In this figure, the numerical profiles are shifted to match the central part of the shock front. The initial slope of the shock is very similar for the TCE and QK models. Both chemistry models slightly underpredict the experimental slope, which is in fact close to the non-reacting case. This may be an indication that TCE and QK models overpredict the number of dissociation reactions inside the shock. They underpredict the maximum vibrational temperature due to the same reason. Note that the QK model is somewhat closer to the experimental value of $\sim$4,300 K, although the aftershock decrease in vibrational temperature is slower in the computation than in the experiment. This may indicate that more dissociation occurs in the actual flow than predicted in the simulation, likely due to the impact of O_2+O reactions. Further downstream, the experimental values are closer to the ones predicted with the TCE model.

M=13.4 SHOCK WAVE

For the M=9.3 flow considered in the previous section, the dissociation becomes important after the translational and rotational temperatures have peaked. In the second test case under consideration, M=13.4, the chemical reactions are a key factor even before the translation-rotation equilibrium is reached. This is clearly seen in Fig. 4, where gas density,

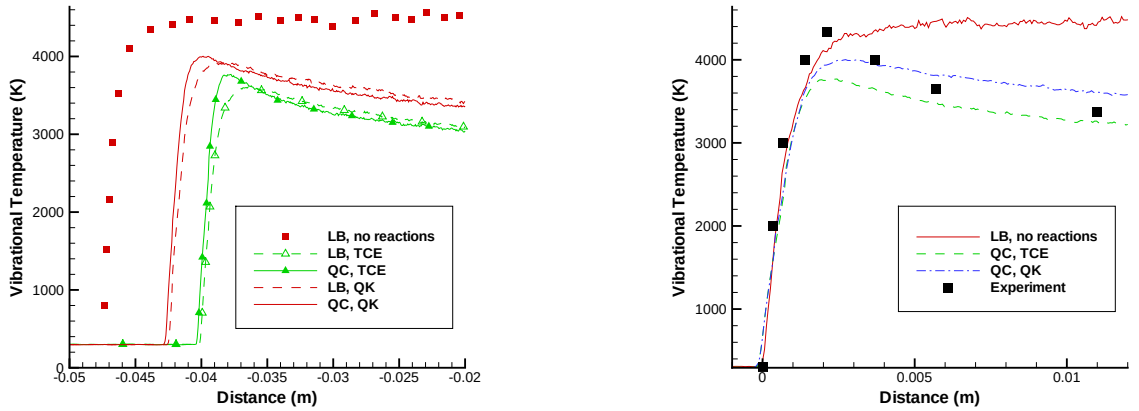

FIGURE 4. Vibrational temperature profiles for M=9.3: the effect of numerical model (felt) and comparison with measurement [4] (right).

bulk velocity, and atomic oxygen mole fraction (Fig. 4, left) and mode temperatures (Fig. 4, right) are presented along the stagnation streamline. By the time the flow velocity is near its after-shock value, and the rotational temperature reaches its maximum, the atomic oxygen mole fraction reaches 0.3, which is almost an order of magnitude larger than that for the M=9.3 case. The oxygen mole fraction quickly reaches 0.5 and then the rate of increase significantly drops, as the gas temperature decreases from over 8,000 K to less than 4,000 K. Similar to M=9.3 flow, the bulk flow velocity slowly decreases from it after-shock value to about 0 near the wall. The gas density increases by about a factor of 20 behind the shock wave. Note that significantly larger translational and rotational temperatures, as compared to the M=9.3 case, cause a much faster vibrational relaxation, with vibrational mode equilibrating with the other two shortly after the maximum vibrational temperature has been reached. Further temperature decrease is relatively small, from about 4,000 K at the merging point of vibrational and translational temperatures to ∼3,600 K near the wall (X=0. not shown here).

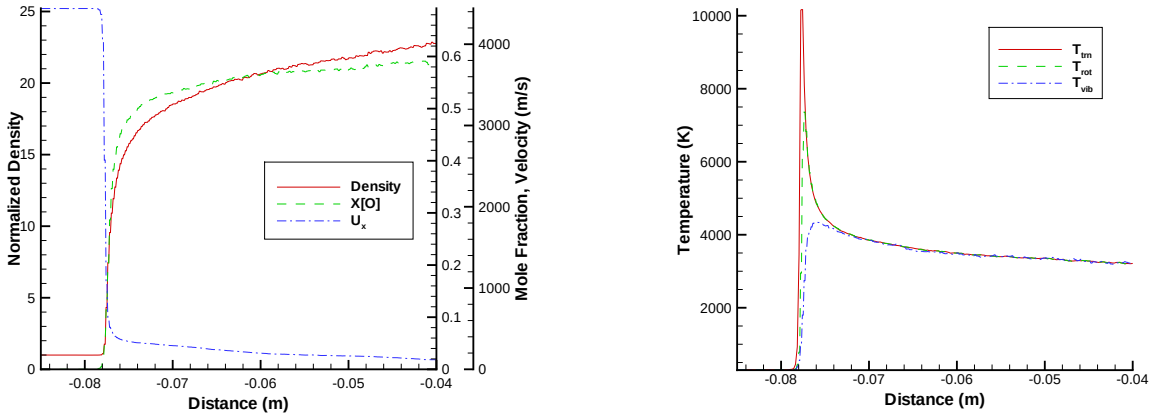

FIGURE 5. Gas macroparameters for M=13.4, computed with LB and TCE models.

Finally, let us compare the computed and measured vibrational temperatures for the M=13.4 case. The comparison is presented in Fig. 6, where the results of three different models of chemical reactions are shown. For all reaction models, the QC model of vibrational relaxation was used. One important conclusion that may be drawn from these results is that both models that do not take into account vibration-dissociation favoring, TCE and QK, largely underpredict vibrational temperature behind the shock, with the maximum difference of almost 2,000 K. The difference in the relaxation zone is about 1,000 K. The main reason for the difference is a significant overprediction of dissociation

reaction rates by models that do not consider vibrational favoring (see [23] for more detail). Note that the profiles for the TCE and QK models are fairly close, with maximum $T - vib$ for the TCE model being about 200 K lower (this is similar to the low-velocity case). The state-specific model that takes into account the dependence of reaction rate on the separation of vibrational and translation-rotational temperatures, predicts the maximum vibrational temperature very well. The after-shock relaxation is slower for that model due to underprediction of the number of O_2+O dissociation reactions. The after-shock plateau of about 4,500 K for the state-specific model is close to the corresponding experimental value.

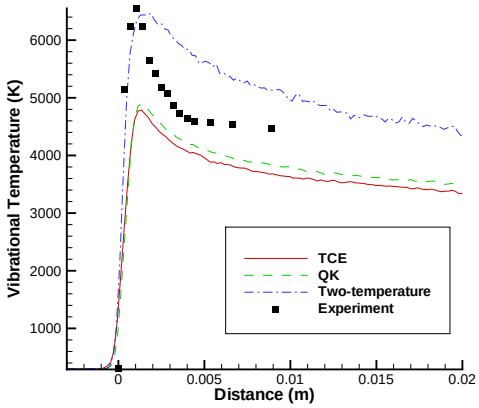

FIGURE 6. Comparison between computed and measured [4] vibrational temperature profiles for a M=13.4 shock.

CONCLUSIONS

Most validation studies for dissociation models either adjust the overall (equilibrium limit) dissociation rate coefficient as one of the adjustable parameters or simulate conditions where the degree of vibration-translation nonequilibrium is not known. The measurements from [3] validate the vibrational relaxation models used. They also allow a rare opportunity to independently fix the value of the equilibrium limit dissociation rate coefficient and simultaneously know the value of the vibrational temperature through the shock. Thus, the nonequilbrium vibration-dissociation coupling aspects of a given model can be validated. Significant work remains to be done on this comparison case, such as checking the role of recombination, investigating the range of validity of the assumed O_2-O rate parameters used, and simulating addition Mach number cases. The preliminary results presented here are very encouraging and indicate the important role of vibrational favoring for a diatomic dissociation reaction model.

ACKNOWLEDGMENTS

The work was supported in part by the Air Force Office of Scientific Research.

REFERENCES

1. G.A. Bird, *Molecular Gas Dynamics and the Direct Simulation of Gas Flows.* Clarendon Press, Oxford, 1994.
2. G.A. Bird, "Monte-Carlo simulation in an engineering context," In *Rarefied Gas Dynamics*, 1981, Vol. 74, pp. 239-255, ed. S. Fisher, Progress in Astronautics and Aeronautics.
3. I. E. Zabelinskii, L.B. Ibraguimova, O.P. Shatalov, "Measurement of vibrational temperature of oxygen behind the shock wave in strong thermal and chemical nonequilibrium," Mekhanika Zhidkosti i Gaza, 2010, Vol. 3, pp. 159-167 (in Russian).
4. L.B. Ibraguimova, A.L. Sergievskaya, O.P. Shatalov, Yu.V. Tunik, I. E. Zabelinskii, "Investigation of Oxygen Dissociation and Vibrational Relaxation at Temperatures 4000 - 10800 K," 28th Rarefied Gas Dynamics Symposium, Zaragoza, Spain, July 2012.

5. M.S. Ivanov, G.N. Markelov, S.F. Gimelshein, “Statistical simulation of the transition between regular and Mach reflection in steady flows,” Computers and Mathematics with Applications, Vol. 35, No. 1-2, 1998, pp. 113-126.
6. M. Capitelli, C. Gorse, S. Longo, D. Giordano, “Collision Integrals of High-Temperature Air Species,” *Journal of Thermophysics and Heat Transfer*, 2000, Vol. 14, No. 2, pp. 259-268.
7. S.F. Gimelshein, I.D. Boyd, M.S. Ivanov, “DSMC Modeling of Vibration-Translation Energy Transfer in Hypersonic Rarefied Flows,” *AIAA Paper 99-3451*, Norfolk, VA, June 1999.
8. J.G. Parker, “Rotational and vibrational relaxation in diatomic gases,” *Phys.Fluids*, 1959, Vol. 2, No. 4, pp. :449-462
9. C. Borgnakke, P.S. Larsen, “Statistical collision model for Monte Carlo simulation of polyatomic gas mixture,” *J. Comp. Phys.*, 1975, Vol. 18, pp. 405-420.
10. F. Bergemann, I.D. Boyd, “DSMC simulation of inelastic collisions using the Borgnakke-Larsen method extended to discrete distributions of vibrational energy,” In *Rarefied Gas Dynamics: Theory and Simulations*,, 1995, Vol. 158, pp. 174-183, ed. BD Shizgal, DP Weaver, Progress in Astronautics and Aeronautics.
11. R.C. Millikan, D.R White, “Systematics of Vibrational Relaxation,” *J. Chem. Phys.*, 1966, Vol. 39, No. 12, pp. 3209-3213.
12. C. Park, “Problems of Rate Chemistry in the Flight Regimes of Aeroassisted Orbital Transfer Vehicles,” *Progr. in Astronautics and Aeronautics*, Vol. 6, AIAA, New York, 1985, pp. 511-537.
13. S.F. Gimelshein, M.S. Ivanov, G.N. Markelov, Yu.E. Gorbachev, “Statistical simulation of nonequilibrium rarefied flows with quasiclassical vibrational energy transfer models,” *Journal of Thermophysics and Heat Transfer*, Vol. 12, No. 4, 1998, pp. 489-495.
14. S.F. Gimelshein, N.E. Gimelshein, D.A. Levin, M.S. Ivanov, I.J. Wysong, “On the use of chemical reaction rates with discrete internal energies in the direct simulation Monte Carlo method,” *Physics of Fluids*, Vol. 16, No. 7, 2004, pp. 2442-2451.
15. G.A. Bird, “A Comparison of Collision Energy-Based and Temperature-Based Procedures in DSMC,” 26th International Symposium on Rarefied Gas Dynamics, *AIP Conf. Proc.*, 2008, Vol. 1084, 245-250.
16. M.A. Gallis, R.B. Bond, J.R. Torcyznski, “A Kinetic-theory Approach for Computing Chemical Reaction Rates in Upper Atmosphere Hypersonic Flows,” *J. Chem. Phys.*, 2009, Vol. 131, 124311.
17. Ye.A. Bondar and M.S. Ivanov. “DSMC Dissociation Model Based on Two-Temperature Chemical Rate Constant,” *AIAA Paper 2007-0614*, 2007.
18. N.M. Kuznetsov, *Kinetics of Unimolecular Reactions*, Nauka, Moscow, 1982 (in Russian).
19. B.L. Haas, I.D. Boyd, “Models for vibrationally favoured dissociation applicable to a particle simulation, *AIAA Paper 91-0774*, 1991.
20. S.F. Gimelshein, Yu.E. Gorbachev, M.S. Ivanov, G.N. Markelov, “Statistical Simulation of Nonequilibrium Rarefied Flows with Quasiclassical VVT Transition Models,” *AIAA Paper 97-2585*, 1997.
21. Ye. Bondar, G. Markelov, S. Gimelshein, M. Ivanov, “Numerical Modeling of Near-Continuum Flow over a Wedge with Real Gas Effects,” *Journal of Thermophysics and Heat Transfer*, 2006, Vol. 20, No. 4, pp. 699-709.
22. S.F. Gimelshein, M.S. Ivanov, S.V. Rogasinsky, “Investigation of shock wave structure by majorant cell and free cell schemes of DSMC,” *Proc. XVII Intern. Symp. on Rarefied Gas Dynamics,*’ Aachen, 1991. pp. 718-726.
23. I. Wysong, S. Gimelshein, N. Gimelshein, W. McKeon, F. Esposito, “Reaction Cross Sections for Two DSMC Models: Accuracy and Sensitivity Analysis,” *Physics of Fluids*, 2012, Vol. 24, 042002.